Polarization-Insensitive Dielectric Metamaterials Absorber for Near-Unity UV-Light Trapping in Monolayer Graphene

Yinong Xie
Xiamen University
Xueying Liu
Xiamen University
Yijun Cai
Xiamen University of Technology
Jinfeng Zhu (nanoantenna@hotmail.com)
Xiamen University https://orcid.org/0000-0003-3666-6763

Nano Express

Keywords: Polarization-insensitive, Dielectric metamaterials absorber, Two-dimensional material, UV-light trapping, Monolayer graphene, Dual-band absorber

Posted Date: December 2nd, 2020

DOI: https://doi.org/10.21203/rs.3.rs-117470/v1

Abstract

With the aim of improving UV light trapping capability in monolayer graphene, a metamaterials absorber is proposed, which exhibits the polarization-insensitive feature due to the geometrical symmetry. Through the functional combination of magnetic resonance and UV mirror, the absorption of unpolarized UV light in monolayer graphene can reach 99.5% under normal incidence. The absorption enhancement is induced by the magnetic resonance mode between the dielectric silica nanomesh and the calcium fluoride base layer. The effects of geometric parameters on the absorption spectra are systematically investigated. By optimizing the metamaterials design, two distinct resonant absorption peaks can be excited simultaneously for monolayer graphene. Our work paves the way for applications on high-performance UV metamaterials devices by using two-dimensional materials.

1. Introduction

In recent years, graphene has become one of the most popular two-dimensional (2D) materials from UV to terahertz ranges due to its fast and broadband optical response [1–5], high carrier mobility, extraordinary band structure, and unique mechanical strength and flexibility [6–9]. Within the spectral range from mid-infrared to terahertz, graphene supports a robust plasmonic response, which significantly enhances the light-graphene interaction. However, in the range from UV to near-infrared (NIR), due to the absence of plasmonic response, monolayer graphene can only absorb a very tiny fraction of the normal incident light (~ 2.3% for the visible-NIR range, and less than 9% for the UV range [10, 11]). Several studies have used graphene with multiple atomic layers to improve the absorption efficiency. The superior performance of graphene as a 2D material will undoubtedly degrade, such as photonic and electron conduction efficiencies [12–14].

Therefore, numerous methods have been intensively studied to strengthen the interaction between monolayer graphene and the incident light, such as configurations with subwavelength-scale patterning inside graphene layers [15, 16]. However, they will not only makes manufacturing more complicated and expensive, but also cause irreversible damage to the electronic and photonic properties of monolayer graphene, whose band structure is very sensitive to atom-scale damage and environmental contaminant.

Notably, unlike the conventional studies of graphene from visible to terahertz spectrum range, the many-body effects of graphene should be taken into account for the high excitation energy of UV light [17]. Graphene and metals in the UV band exhibit totally different properties from those in the longer wavelength range. Precise fabrication of nanoscale features applied on graphene with shorter wavelength range might be much more difficult, so a series of new material and structural engineering are required for trapping UV light in the unpatterned monolayer graphene. A previous study has achieved high optical absorption in graphene by using an unpatterned graphene/medium/metal structure [18]. However, the configuration required specific angle control and polarization manipulation for the incident light.

In order to increase the absorption efficiency of UV light in graphene under normal incidence, metamaterials based on periodic Al nanostructured arrays have been developed to excite the plasmon within the UV spectral range [19, 20]. Unfortunately, most of the incident energy is dissipated in the lossy Al due to the considerable inherent loss of metal. Several periodic dielectric grating arrays are used to trap light for total absorption. However, these efforts mainly focused on the infrared range and require additional polarization manipulation[21, 22]. Therefore, a metamaterials absorber for enhancing UV light-graphene interaction with polarization-insensitive property is quite in demand.

In this work, we propose a graphene-based UV metamaterials absorber with near-unity optical absorption inside graphene. It consists of all-dielectric materials except for graphene and possesses the characteristic of polarization independence. We conduct a systematic investigation on the geometric design, material selection, and polarization properties for the configuration of proposed absorber in the UV band. After rigorous structural optimization, the absorption of UV light inside graphene can be increased up to 99.5%, which is more than 10 times larger than that inside suspended graphene. Moreover, the electric and magnetic field distributions are investigated to reveal the absorption mechanism.

2. Structure And Design

In this work, we propose a graphene-based UV metamaterials absorber with near-unity optical absorption inside graphene. It consists of all-dielectric materials except for graphene and possesses the characteristic of polarization independence. We conduct a systematic investigation on the geometric design, material selection, and polarization properties for the configuration of proposed absorber in the UV band. After rigorous structural optimization, the absorption of UV light inside graphene can be increased up to 99.5%, which is more than 10 times larger than that inside suspended graphene. Moreover, the electric and magnetic field distributions are investigated to reveal the absorption mechanism.

The all-dielectric photonic structure is mainly composed of the following four parts as plotted in Fig. 1: the central symmetric SiO_2 nanomesh is prepared on the surface of the calcium fluoride (CaF_2) layer, the monolayer graphene as the absorption material is transferred and sandwiched between them. The laminated structure with almost perfect reflection is formed by the dielectric layer with high refractive index layer (ZrO_2) and low refractive index (Na_3AlF_6), while the transparent substrate (SiO_2) also acts as a part of the UV mirror. The geometry of the metamaterials is described by t_1, w, t_2, and p as shown in Fig. 1. The numerical simulation is conducted by the commercial software COMSOL Multiphysics. The periodic boundary conditions are adopted in the x-axis and y-axis, respectively. The normal incident light is introduced from above along z-axis direction. In our design, the dielectric layers of SiO_2, CaF_2, ZrO_2, Na_3AlF_6 and substrate are assumed to be nonmagnetic ($\mu = \mu_0$) and optically lossless with the refractive index of 1.48, 1.45, 2.60, 1.33 and 1.48, respectively. The UV mirror is optimized with 5 layers of ZrO_2 (26.9 nm thick) and 4 layers of Na_3AlF_6 (52.6 nm thick) for UV nearly-total reflection under normal

incidence. Based on the many-body effects in the UV range, monolayer graphene could be considered as a two-dimensional conductive surface with a dispersive conductivity σ, which can be described by the equations of the Fano model [23],

$$\sigma(\lambda) = \frac{\sigma_{CB}(\lambda) \cdot (q + \varepsilon)}{1 + \varepsilon^2} \quad (1)$$

$$\varepsilon = \frac{h_c / \lambda - E_r}{\Gamma / 2} \quad (2)$$

where λ, h_c and c represent the free space wavelength, Plank constant and the speed of light in vacuum, respectively. $\sigma_{CB}(\lambda)$ is the continuum background from the calculation of a many-body system, which represents the response away from the singularity [24]. The Fano parameter q= -1 denotes the intensity of the excitonic transition to the unperturbed band transitions and the asymmetry of the conductivity line shape. ε is the normalized energy by width Γ=0.78 eV relative to the resonance energy E_r = 5.02 eV of the perturbed exciton. Optical simulations are performed to optimize the parameters of the structure for complete UV light absorption.

3. Results And Discussion

Initially, we investigate the polarization dependence of incident light. We compared the absorbance of nanograting and nanomesh structures under *s*-polarized light and *p*-polarized light incidence, respectively, as shown in Fig. 2 (a) (the schematic drawings of the two structures are shown in the inset). When the geometric parameters shown in the caption are adopted, the nanograting structure exhibits relatively high absorbance under *s*-polarized incidence. However, the absorbance is rather low under *p*-polarized light incidence, which indicates an obvious polarization dependence. In contrast, the nanomesh structure with the same geometric parameters has a relatively high UV absorbance inside graphene for both *s*-polarized and *p*-polarized incidence, which is attributed to the central symmetry of the nanomesh structure. The maximum UV absorbance peak is larger than 80% at λ = 273 nm and the absorbance spectra of the two polarizations are identical, which solves the problem of polarization dependence of the nanograting structure. Moreover, as shown in Figure. 2 (b), owing to the polarization dependence of grating structure, the absorbance inside graphene is only 65% at 273 nm under non-polarization incidence. In order to reveal the mechanism of the absorption enhancement, the magnetic field and electric field distribution of the nanomesh structure is plotted in the Figures. 2 (c) and 2 (d). A remarkable magnetic dipole resonance appears around the graphene layer at λ = 273 nm while the off-resonance state is observed at λ = 332 nm. For an optimized structure, the presence of magnetic resonance induces the concentrated electric field parallel to the graphene layer and contributes to the enhanced UV absorption inside graphene as shown in the Figure.2 (d). Moreover, the increase of UV absorption can also be further explained by the calculation of optical absorption. In graphene, the optical absorption is determined by the following equation [25],

$$A(\lambda)=\frac{4\pi c}{\lambda}\cdot n(\lambda)\cdot k(\lambda)\cdot\int_V|E_l|^2\,dV \quad (3)$$

where c and λ are the speed and wavelength of light in free space, V is the volume of graphene, and E_l is the local electric field. Based on Eq. (3), the absorbance is proportional to the square of local electric field intensity. Apparently, the absorbance of UV light inside graphene is significantly improved at λ = 273 nm due to the strong enhancement of in-plane electric field.

We next consider the influence of changing the thickness of the SiO_2 nanomesh layer on the UV absorption. With the increase of t_1 from 10 nm to 150 nm as shown in Figure. 3(a), the maximum UV absorbance peak exhibits a redshift from 268 nm to 282 nm due to the increment of the effective resonance wavelength of the magnetic dipole. When t_1 is set at a low value of 10 nm, the maximum absorbance is relatively low, because the magnetic resonance mode (MRM) is mainly confined inside the CaF_2 layer and the corresponding electric field enhancement is more concentrated in this layer. Compared with the thickness of 10 nm, the use of 30 nm for t_1 results in the location change of MRM (as shown in Figure. 3(b)), which induces much stronger in-plane electric field concentration on the graphene surface. Along with the further increase of t_1, there is an optimum value of 100 nm, for which the in-plane electric field induced by the MRM (as shown in Figure. 3(b)) is highly confined on the graphene surface leading to the highest UV absorption of 99.5% at λ = 278 nm. As t_1 changes to 150 nm, the MRM moves gradually away from the surrounding environment of graphene surface, which leads to the decrease of maximum UV absorption rate.

We further consider the effect of w variation on the absorption of graphene, as demonstrated in Figure. 3(c). In this discussion, we fix the period. When the filling factor determined by w/p is small enough, the intensity of the localized electric field parallel to the graphene surface is relatively weak, which leads to an insufficient absorption enhancement. As w becomes larger, the absorbance increases significantly. For the width ranging from 50 nm to 90 nm, the maximum absorbance ratios remain above 99%. When w = 90 nm, a near-unity absorption is achieved at λ = 278 nm. As w increases and approaches p, the filling factor w/p is almost equal to 1. Electric fields cannot be concentrated due to the attenuation of MRM in the nanostructure, resulting in the dramatic reduction of UV absorption. In addition, as w increases from 10 nm to 130 nm, the maximum absorption peak shifts from 264 nm to 284 nm. We can also observe the filed distribution to have a better understanding of the absorption enhancement, as shown in the Figure. 3(d). When w is set as 10 nm, there is little UV absorption enhancement, because the MRM cannot be effectively excited due to the tiny filling factor. As w is optimized to the value of 90 nm, there is an obvious MRM leading to the significant concentration and enhancement in-plane electric field in the graphene surface.

After discussing the effects on changing the stripe thickness and width of nanomesh structure, we investigate the influence of the nanostructure period p and the CaF_2 thickness t_2 on UV absorption of graphene as demonstrated in Figure. 4. The effect of changing p on the UV absorption is shown in Figure.

4(a). When p is chosen as 180 nm, the magnetic dipole resonance cannot be effectively excited, resulting in a relatively low absorbance. With the increase of p, the magnetic resonance mode is excited and strengthened, and the absorption rate increases dramatically. The magnetic dipole mode is not completely excited until p increases to 220 nm. Meanwhile, the maximum in-plane field on the graphene surface is induced and results in the corresponding maximum absorption rate of 99.5% at λ = 278 nm. With the further increase of p, the absorption peak has a red shift and the absorbance slightly drops down. These results indicate that there is an optimum value of the period for the maximum UV absorption peak of graphene.

We finally study the thickness influence of CaF_2 on UV absorption. As shown in Figure. 4 (b), when t_2 changes from 80 nm to 135 nm, the resonant wavelength has a redshift from 262 nm to 282 nm. The value of redshift for a unit change of thickness is significantly larger than that influenced by the change of t_1 (as shown in Figure. 3(a)). This is because the magnetic resonance has a dominant mode region in the CaF_2 layer, whose change of thickness has a more remarkable effect on the position of absorption peak. In view of this, when we further increase t_2 to the value of 205 nm, the interior interference effect induces two UV absorbance peaks over 90% at the wavelengths of 295 nm and 257 nm, respectively, where the first one is attributed to the low-order magnetic resonance and the second one is induced by the interference in the CaF_2 layer. This effect provides a new way for the application of UV double resonance spectroscopy [26, 27].

4. Conclusion

In summary, we propose a polarization-independent near-unity metamaterials absorber in the UV range based on the monolayer graphene. The use of all-dielectric materials except for graphene avoids the intrinsic loss inside metal materials. Meanwhile, the use of the UV mirror leads to a higher efficiency of light trapping inside graphene. Due to the electric field enhancement caused by magnetic dipole resonance in monolayer graphene, an optimized metamaterials absorber can achieve a UV absorption rate up to 99.5%. Besides, it reveals an excellent polarization-insensitive property due to the geometrical symmetry, which brings more convenience in practical application of UV absorption. In addition, by adjusting the thickness of the CaF_2 layer and the period of the unit cell properly, two resonances with absorption rates more than 90% can be observed in the spectrum. The proposed absorber greatly enhances the light-matter interaction for near-unity UV absorption in sub-nanometer 2D materials, which has a great potential for the development of high-performance optoelectronic devices in the UV range.

Abbreviations

2D: Two-dimensional

NIR: Near-infrared

CaF_2: Calcium fluoride

MRM: Magnetic resonance mode

Declarations

Availability of data and materials

All data are fully available without restriction.

Competing interests

The authors declare no competing financial interests.

Funding

This work was supported by National Natural Science Foundation of China (U1830116, 62005232); the Open Fund of State Key Laboratory of Applied Optics (SKLAO2020001A15); Fundamental Research Funds for the Central Universities (20720190010).

Authors' contributions

X. Y. and Z. J. conceived the idea and wrote the manuscript. X. Y. and L. X. undertook the simulations. X. Y. analyzed the data. C. Y. and Z. J. supervised the project.

Acknowledgments

Not applicable

References

1. R. Tang, S. Han, F Teng, K Hu, Z Zhang, M Hu and X Fang (2018) Size-Controlled Graphene Nanodot Arrays/ZnO Hybrids for High-Performance UV Photodetectors. Adv. Sci. 51: 1700334.
2. L. Ye, Y. Chen, G. Cai, N. Liu, J. Zhu, Z. Song and Q. H. Liu (2017) Broadband absorber with periodically sinusoidally-patterned graphene layer in terahertz range. Opt. Express 25: 11223-11232.
3. T. Chen, , Y. Lu, Y. Sheng, Y. Shu, X. Li, R. Chang, H. Bhaskaran and J. H. Warner (2019) Ultrathin all-2D lateral Graphene/GaS/Graphene UV photodetectors by direct CVD growth. Acs Appl. Mater. Inter. 11: 48172-48178.
4. H. Lee, D. Yoo, P. Avouris, T. Low, and S. H. Oh (2019) Graphene acoustic plasmon resonator for ultrasensitive infrared spectroscopy. Nat. Nanotechnol. 14: 313-319.
5. J. Zhu, C. Li, J. Y. Ou, and Q. H. Liu (2019) Perfect light absorption in graphene by two unpatterned dielectric layers and potential applications. Carbon 142: 430-437.
6. J. Wang, Y. Hernandez, M. Lotya, J. N. Coleman and W. J. Blau (2009) Broadband nonlinear optical response of graphene dispersions. Adv. Mater. 21: 2430-2435.

7. D. B. Farmer, H. Y. Chiu, Y. M. Lin, K. A. Jenkins, F. Xia and P. Avouris (2009) Utilization of a buffered dielectric to achieve high field-effect carrier mobility in graphene transistors. Nano Lett. 9: 4474-4478.
8. M. I. Katsnelson and K. S. Novoselov (2007) Graphene: New bridge between condensed matter physics and quantum electrodynamics. Solid State Commun. 143: 3-13.
9. Q. Bao and K. P. Loh (2012) Graphene photonics, plasmonics, and broadband optoelectronic devices. ACS Nano 6: 3677-3694.
10. R. R. Nair, P. Blake, A. N. Grigorenko, K. S. Novoselov, T. J. Booth, T. Stauber, N. M. R. Peres and A. K. Geim (2008) Fine structure constant defines visual transparency of graphene. Science 320: 1308-1308.
11. S. Bae, H. Kim, Y. Lee, X. Xu, J. Park, Y. Zheng, J. Balakrishnan, T. Lei, H. R. Kim, Y. Il Song, Y. Kim, K. S. Kim, B. O. zyilmaz, J. Ahn, B. H. Hong and S. Iijima (2010) Roll-to-roll production of 30-inch graphene films for transparent electrodes, Nat. Nanotechnol. 5: 574.
12. M. Koshino (2013) Stacking-dependent optical absorption in multilayer graphene. New J. Phys. 15: 015010.
13. M. Koshino and T. Ando (2009) Electronic structures and optical absorption of multilayer graphenes. Solid State Commun. 149: 1123-1127.
14. P. A. Obraztsov, M. G. Rybin, A. V. Tyurnina, S. V. Garnov, E. D. Obraztsova, A. N. Obraztsov, and Y. P. Svirko (2011) Broadband light-induced absorbance change in multilayer graphene. Nano Lett. 11(4), 1540-1545.
15. C. Berger, Z. Song, X. Li, X. Wu, N. Brown, C. Naud, D. Mayou, T. Li, J. Hass, A. N. Marchenkov, E. H. Conrad, P. N. First and E. H. Conrad (2006) Electronic confinement and coherence in patterned epitaxial graphene. Science 312: 1191-1196.
16. H. Ago, I. Tanaka, C. M. Orofeo, M. Tsuji and K. I. Ikeda (2010) Patterned growth of graphene over epitaxial catalyst. Small 6: 1226-1233.
17. K. F. Mak, L. Ju, F. Wang, and T. F. Heinz (2012) Optical spectroscopy of graphene: From the far infrared to the ultraviolet. Solid State Commun. 152: 1341-1349.
18. J. Zhu, S. Yan, N. Feng, L. Ye, J. Y. Ou and Q. H. Liu (2018) Near unity ultraviolet absorption in graphene without patterning. Appl. Phys. Lett. 112: 153106.
19. R. González-Campuzano, J. M. Saniger and D. Mendoza (2017) Plasmonic resonances in hybrid systems of aluminum nanostructured arrays and few layer graphene within the UV–IR spectral range. Nanotechnology 28: 465704.
20. Y. Cai, Z. Wang, S. Yan, L. Ye and J. Zhu. (2018) Ultraviolet absorption band engineering of graphene by integrated plasmonic structures. Opt. Mater. Express 8: 3295-3306.
21. C. Guo, Z. Zhu, X. Yuan, W. Ye, K. Lliu, J. Zhang, W. Xu and S. Qin (2016) Experimental Demonstration of Total Absorption over 99% in the Near Infrared for Monolayer-Graphene-Based Subwavelength Structures. Adv. Opt. Mater. 4: 1955-1960.

22. Y. Qing, H. Ma, Y. Ren, S. Yu, and T. Cui (2019) Near-infrared absorption-induced switching effect via guided mode resonances in a graphene-based metamaterial. Opt. Express 27: 5253-5263.
23. K. F. Mak, J. Shan and T. F. Heinz (2011) Seeing many-body effects in single-and few-layer graphene: observation of two-dimensional saddle-point excitons. Phys. Rev. Lett. 106: 046401.
24. L. Yang, J. Deslippe, C. H. Park, M. L. Cohen and S. G. Louie (2009) Excitonic effects on the optical response of graphene and bilayer graphene. Phys. Rev. Lett. 103: 186802.
25. Y. Cai, J. Zhu and Q. H. Liu (2015) Tunable enhanced optical absorption of graphene using plasmonic perfect absorbers. Appl. Phys. Lett. 106(4), 043105.
26. E. C. Stanca-Kaposta and J. P. Simons (2011). High-resolution infrared-ultraviolet (IR-UV) double-resonance spectroscopy of biological molecules. Handbook of High-resolution Spectroscopy.
27. M. P. Callahan, B. Crews, A. Abo-Riziq, L. Grace, M. S. de Vries, Z. Gengeliczki, T. M. Holmesc and G. A. Hill (2007) IR-UV double resonance spectroscopy of xanthine. Phys. Chem. Chem. Phys. 9: 4587-4591.

Figures

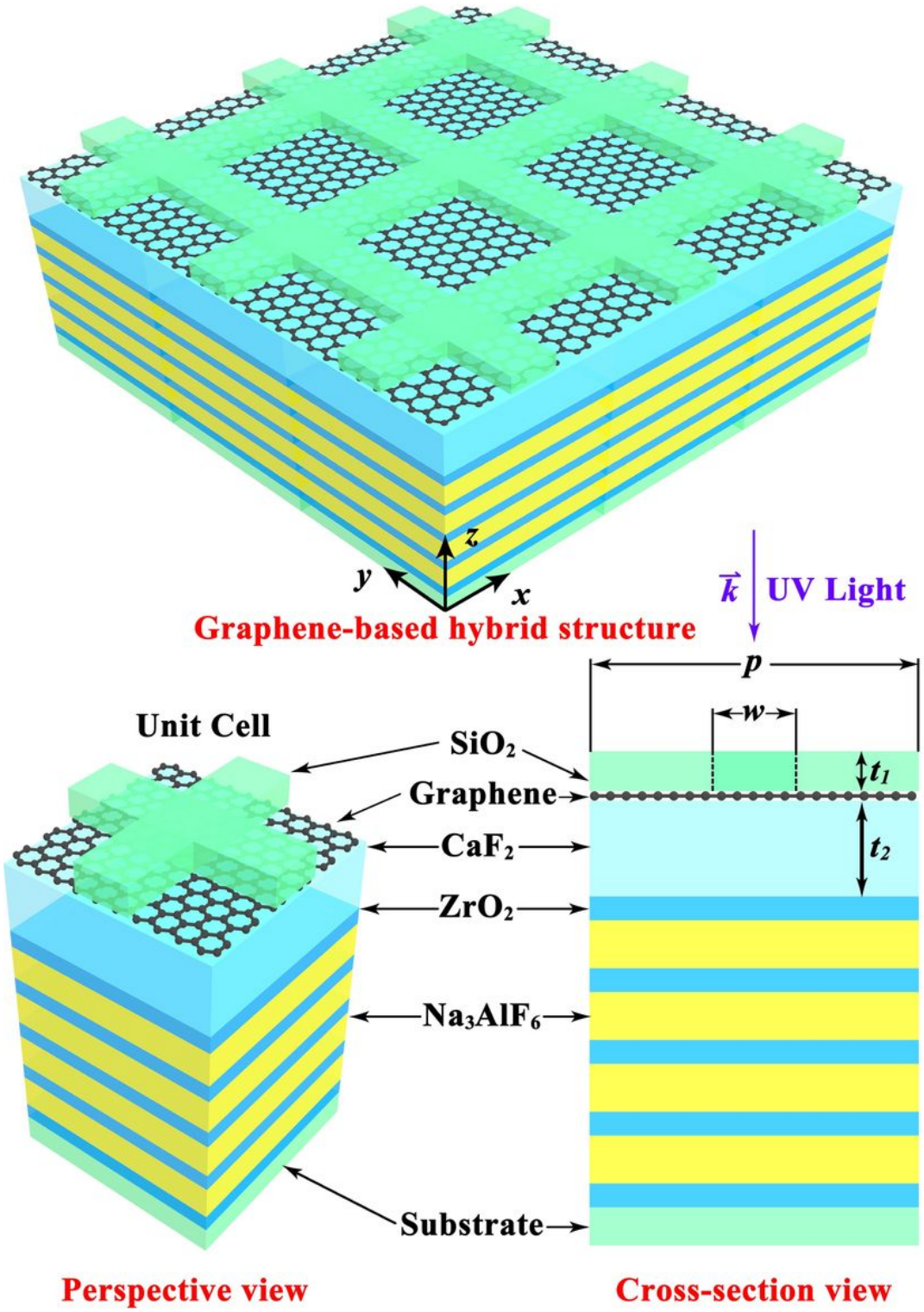

Figure 1

Schematic drawing of the proposed UV absorber based on graphene. The symbols w, p, t1 and t2 represent the width of nanomesh strip, period of nanomesh, thickness of silica nanomesh layer and thickness of CaF2, respectively.

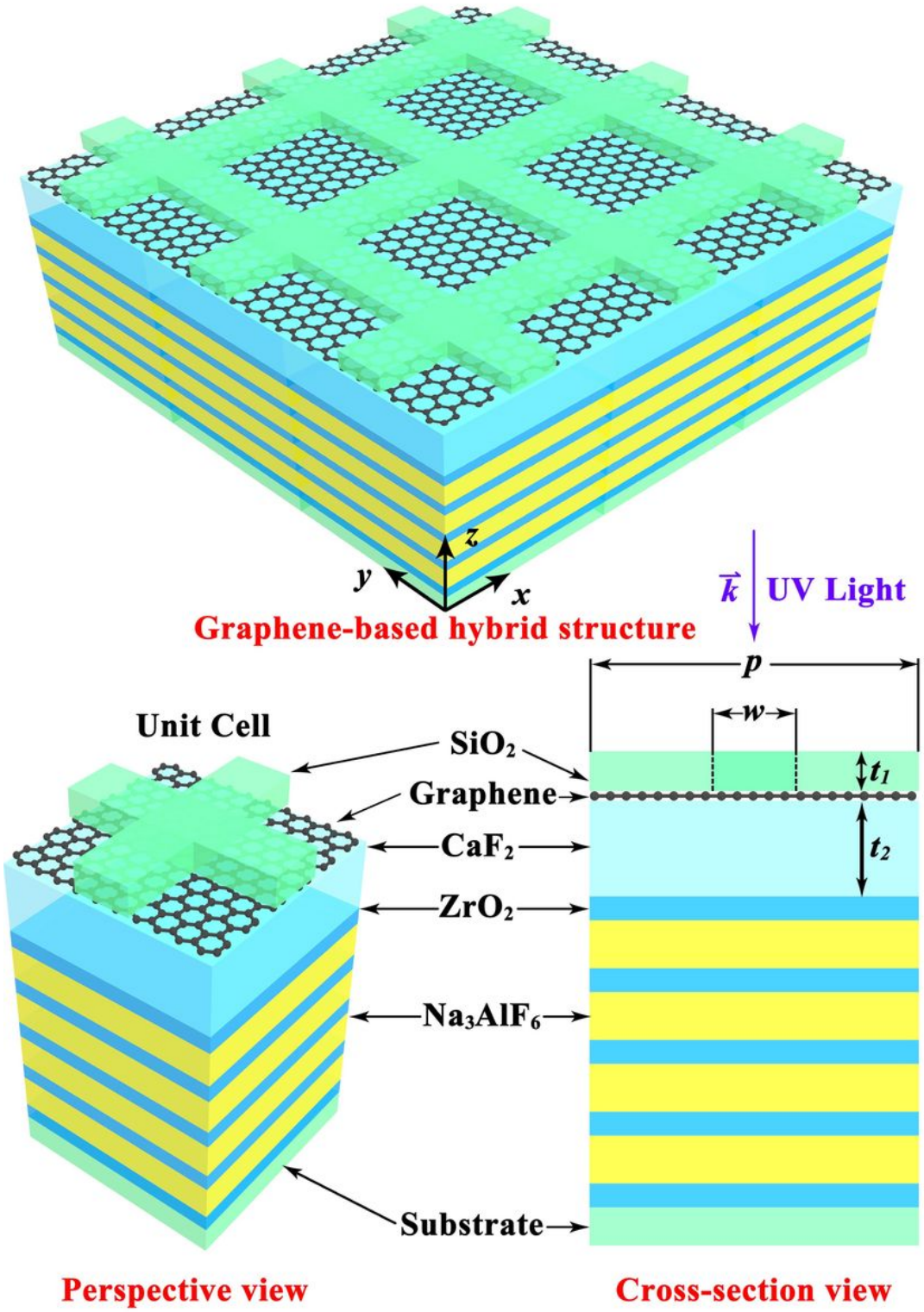

Figure 1

Schematic drawing of the proposed UV absorber based on graphene. The symbols w, p, t1 and t2 represent the width of nanomesh strip, period of nanomesh, thickness of silica nanomesh layer and thickness of CaF2, respectively.

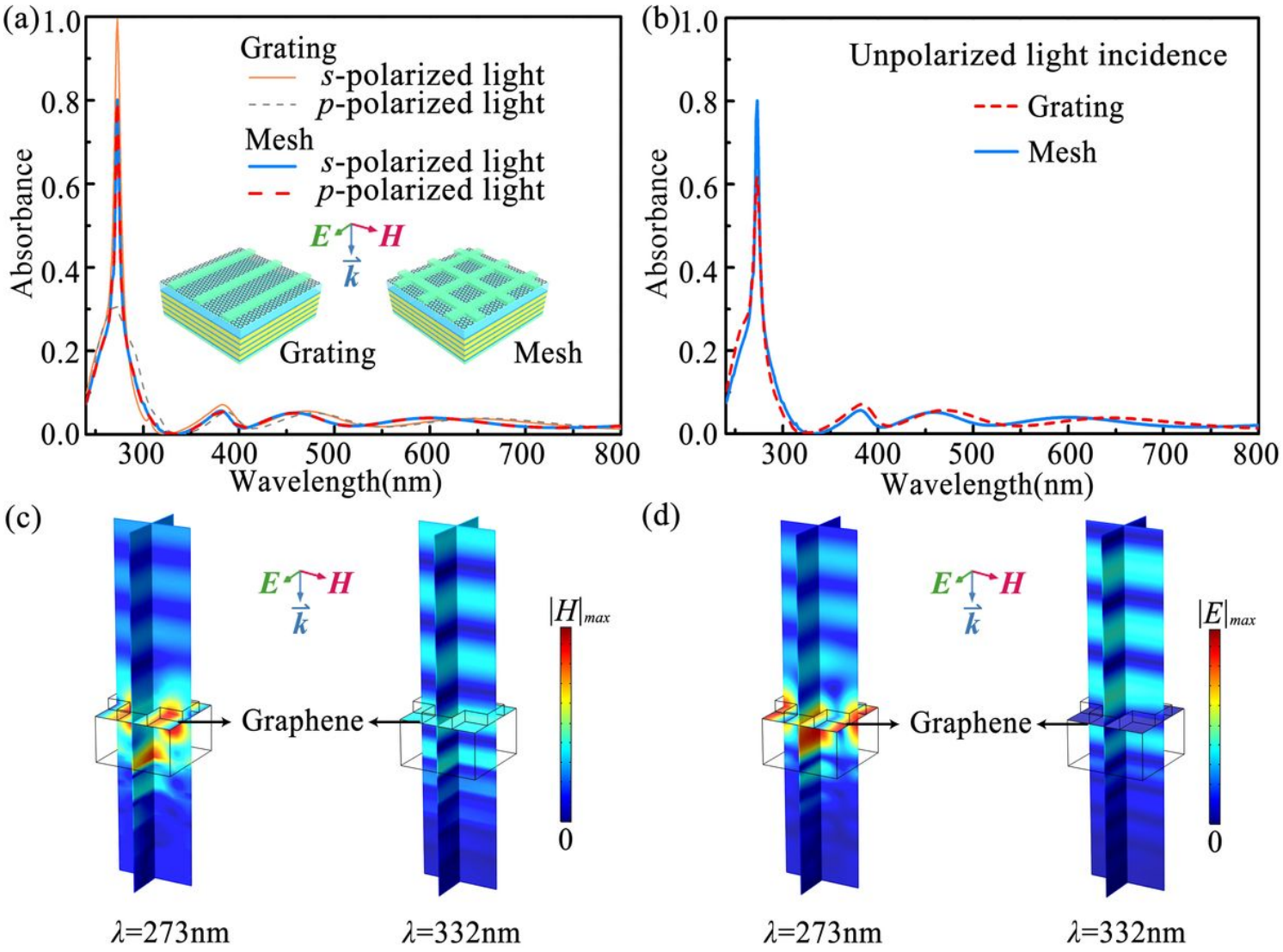

Figure 2

(a) Comparison of absorbance between nanograting and nanomesh structures under different polarizations. (b) Comparison of absorbance between nanograting and nanomesh structures for unpolarized light. (c) Magnetic field distributions and (d) Electric field distributions for w = 111 nm, p = 221 nm, t1 = 30 nm and t2 = 120 nm.

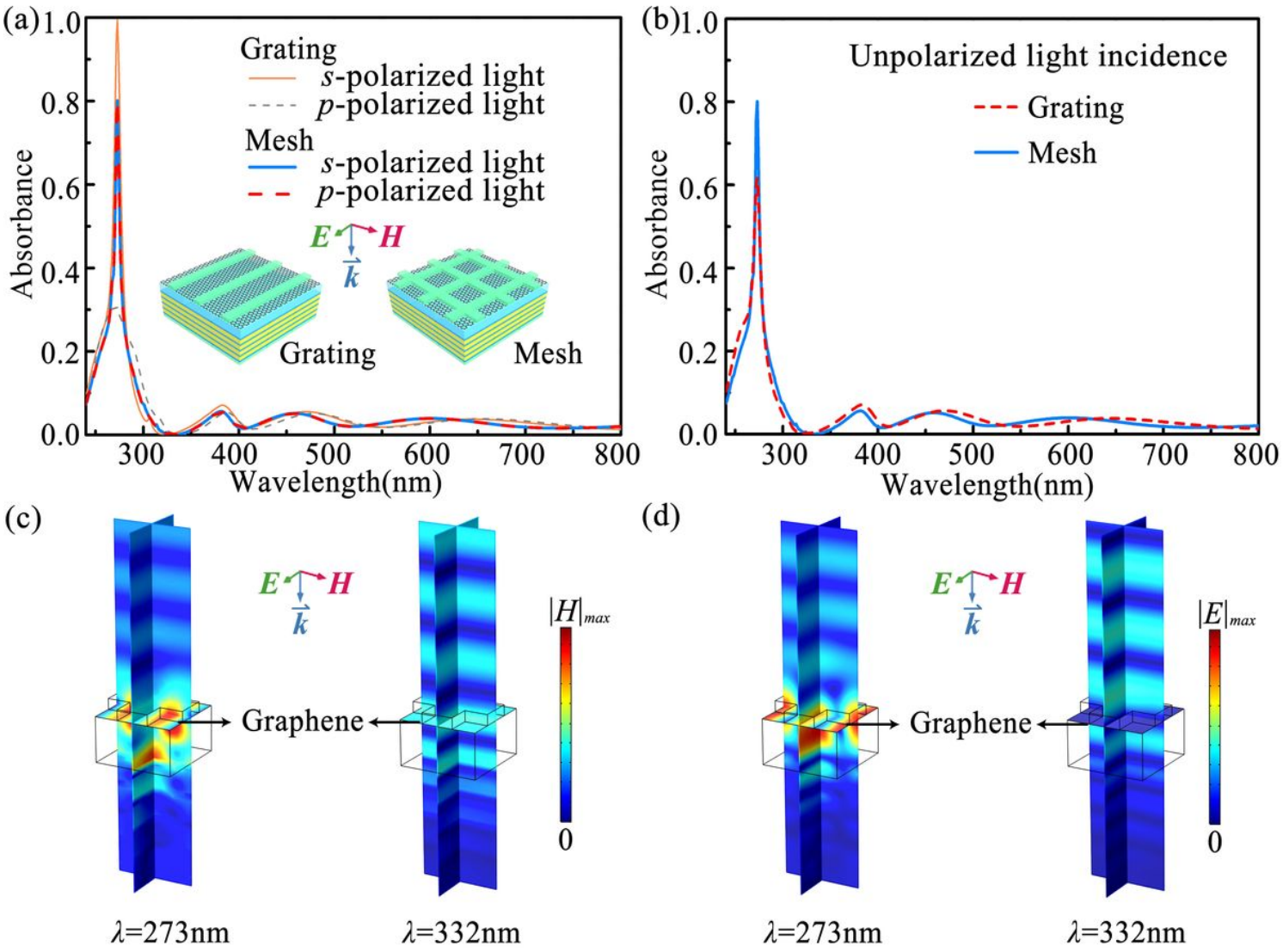

Figure 2

(a) Comparison of absorbance between nanograting and nanomesh structures under different polarizations. (b) Comparison of absorbance between nanograting and nanomesh structures for unpolarized light. (c) Magnetic field distributions and (d) Electric field distributions for w = 111 nm, p = 221 nm, t1 = 30 nm and t2 = 120 nm.

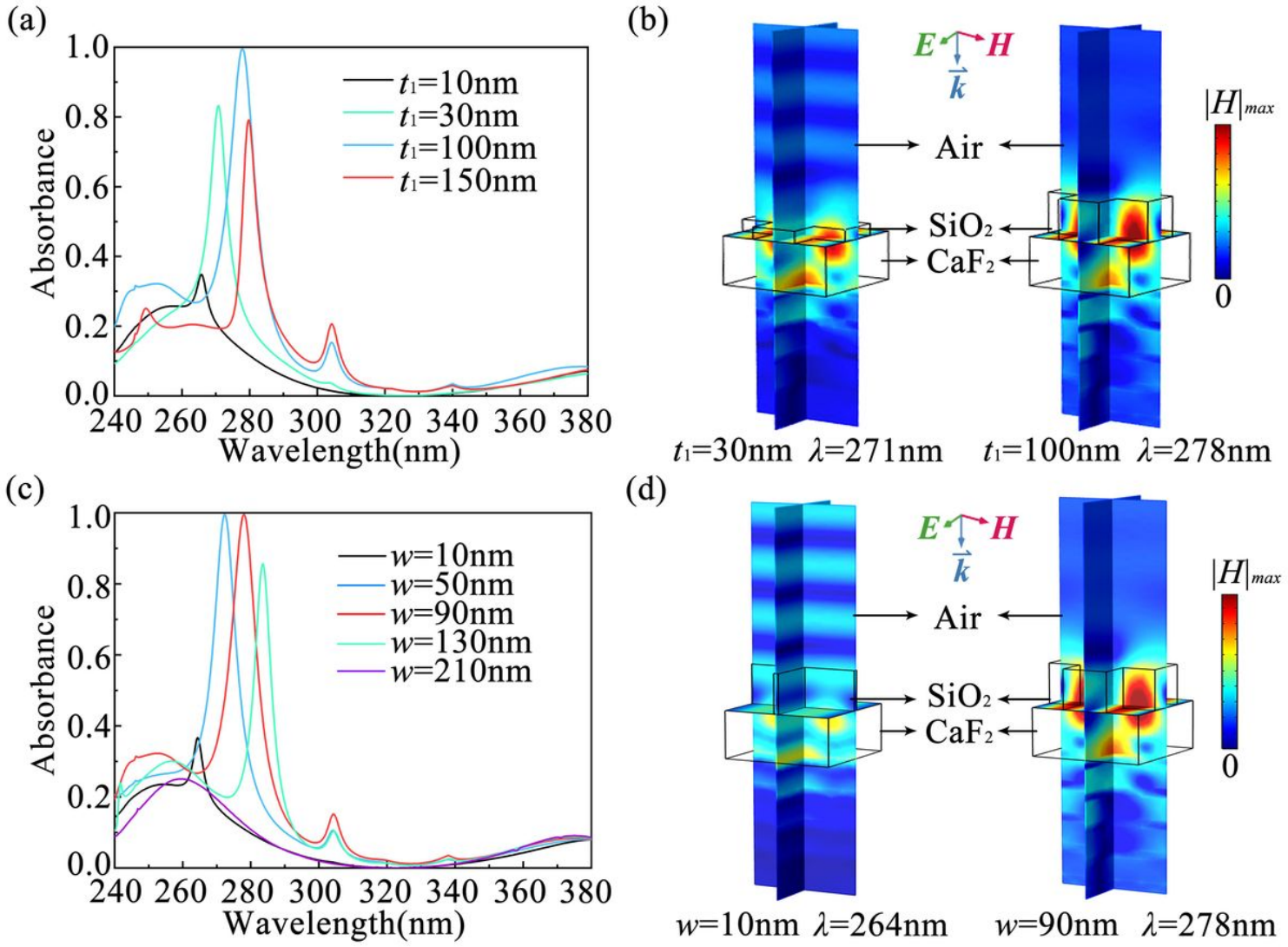

Figure 3

(a) Absorbance of graphene as a function of λ and t1, where p = 221 nm, w = 90 nm and t2 = 120 nm. (b) Comparison of magnetic field distributions under different t1 for p = 221 nm, w = 90 nm and t2 = 120 nm. (c) Absorbance in graphene as a function of λ and w, where p = 221 nm, t1 = 100 nm and t2 = 120 nm. (d) Comparison of magnetic field distributions under different w for p = 221 nm, t1 = 100 nm and t2 = 120 nm.

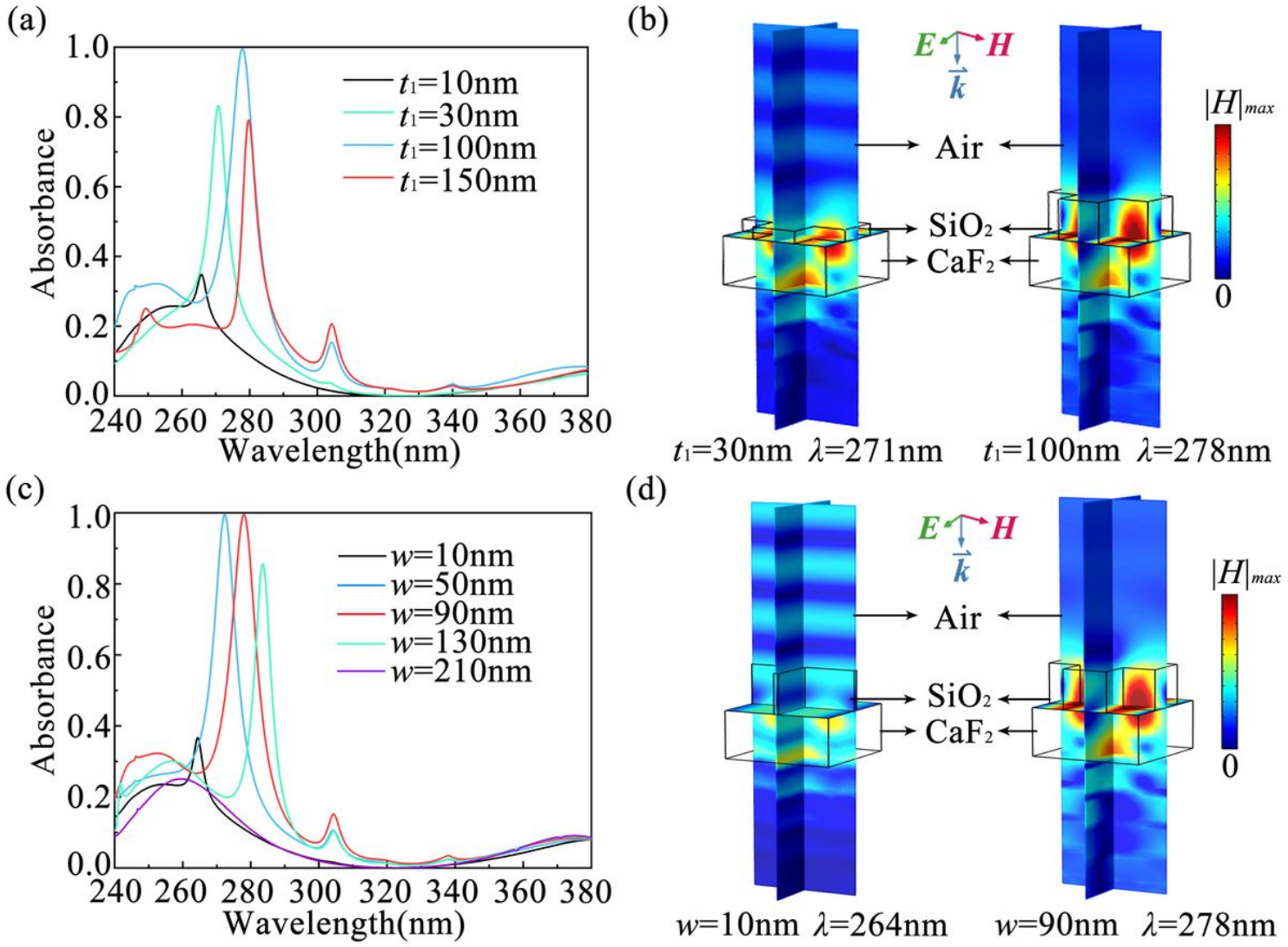

Figure 3

(a) Absorbance of graphene as a function of λ and t1, where p = 221 nm, w = 90 nm and t2 = 120 nm. (b) Comparison of magnetic field distributions under different t1 for p = 221 nm, w = 90 nm and t2 = 120 nm. (c) Absorbance in graphene as a function of λ and w, where p = 221 nm, t1 = 100 nm and t2 = 120 nm. (d) Comparison of magnetic field distributions under different w for p = 221 nm, t1 = 100 nm and t2 = 120 nm.

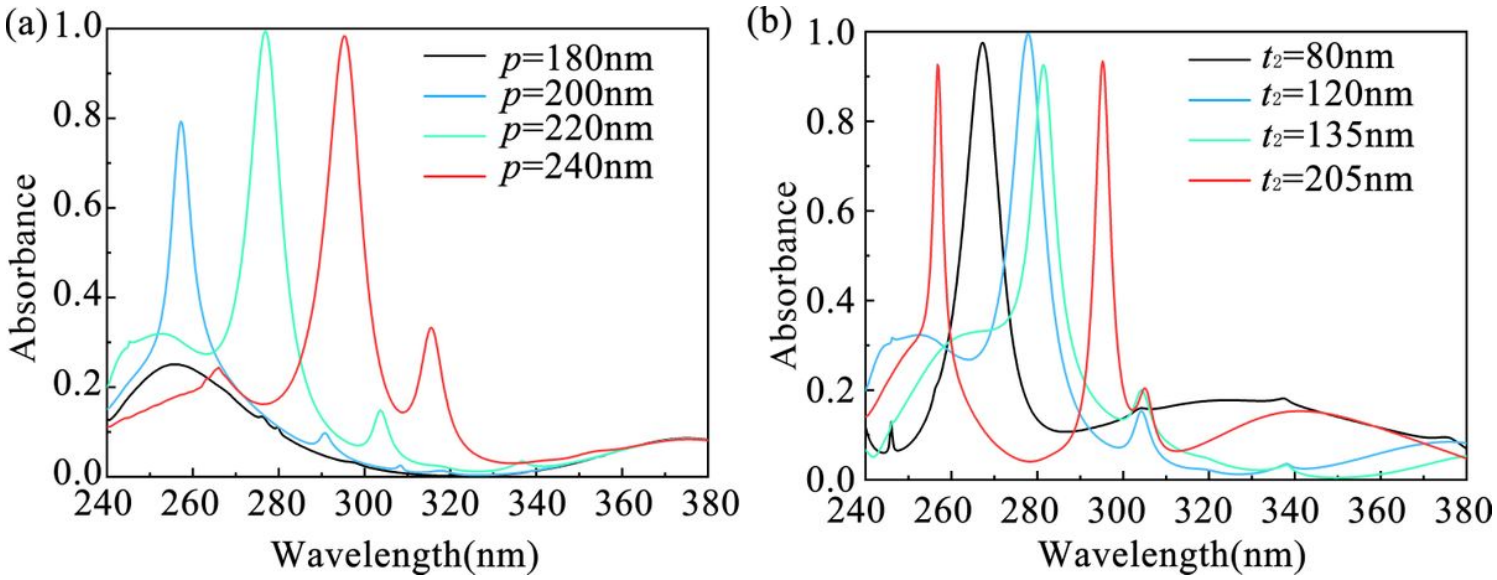

Figure 4

Absorbance in graphene as a function of λ and p, where w = 111 nm, t1 = 100 nm and t2 = 120 nm. (b). Absorbance in graphene as a function of λ and t2, where p = 221 nm, t1 = 29 nm and t2 = 126 nm.

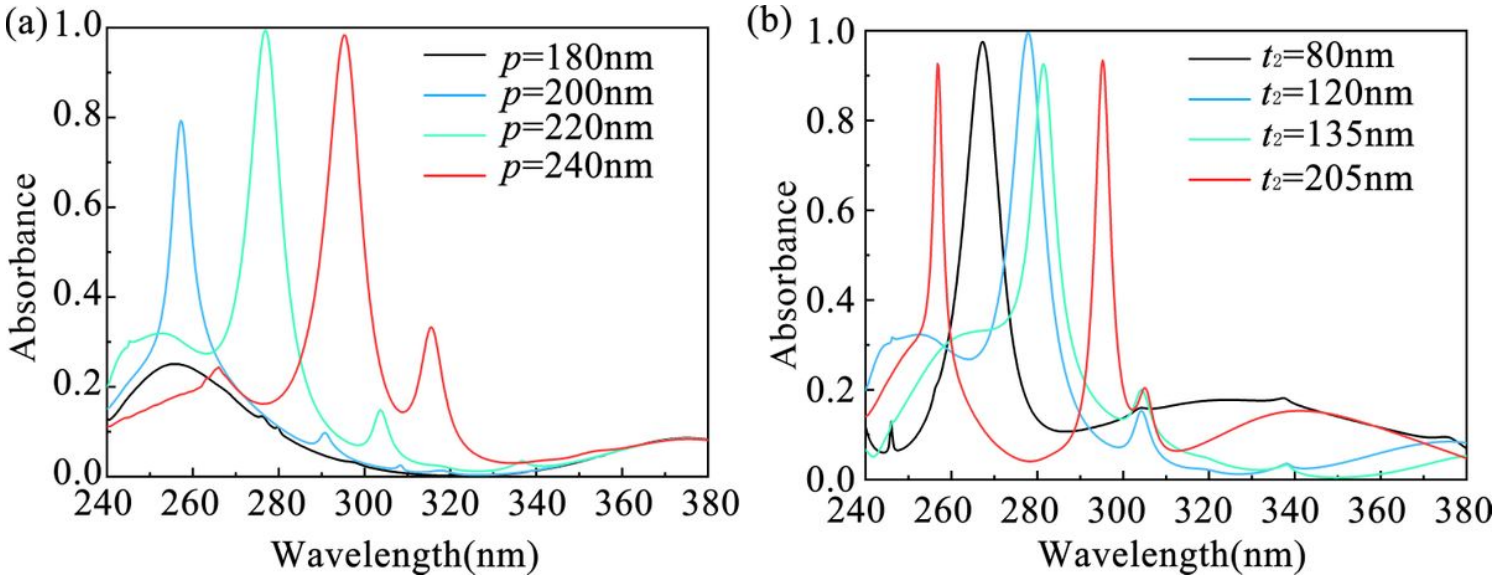

Figure 4

Absorbance in graphene as a function of λ and p, where w = 111 nm, t1 = 100 nm and t2 = 120 nm. (b). Absorbance in graphene as a function of λ and t2, where p = 221 nm, t1 = 29 nm and t2 = 126 nm.